Chemical Engineering Journal 397 (2020) 125519

Contents lists available at ScienceDirect

Chemical Engineering Journal

journal homepage: www.elsevier.com/locate/cej

Plasma-catalytic dry reforming of methane: Screening of catalytic materials in a coaxial packed-bed DBD reactor

J.A. Andersen[a], J.M. Christensen[a], M. Østberg[b], A. Bogaerts[c], A.D. Jensen[a,*]

[a] Department of Chemical and Biochemical Engineering, Technical University of Denmark, 2800 Kgs. Lyngby, Denmark
[b] Haldor Topsøe A/S, Haldor Topsøes Allé 1, 2800 Kgs. Lyngby, Denmark
[c] Research Group PLASMANT, Department of Chemistry, University of Antwerp, 2610 Wilrijk, Belgium

HIGHLIGHTS

- The plasma was found to activate the dry reforming mixture at ambient conditions.
- A CO_2 and CH_4 conversion of ~22% and ~33% was achieved, respectively.
- A large variety of hydrocarbons and oxygenated compounds was detected.
- Methanol was the fifth most selective compound formed.
- SEM-EDS revealed migration of electrode material onto the surface of the packing material.

ARTICLE INFO

Keywords:
Plasma catalysis
Dry reforming of methane
Syngas production
DBD plasma

ABSTRACT

The combination of catalysis with non-thermal plasma is a promising alternative to thermal catalysis. A dielectric-barrier discharge reactor was used to study plasma-catalytic dry reforming of methane at ambient pressure and temperature and a fixed plasma power of 45 W. The effect of different catalytic packing materials was evaluated in terms of conversion, product selectivity, and energy efficiency. The conversion of CO_2 (~22%) and CH_4 (~33%) were found to be similar in plasma-only and when introducing packing materials in plasma. The main reason is the shorter residence time of the gas due to packing geometry, when compared at identical flow rates. H_2, CO, C_2-C_4 hydrocarbons, and oxygenates were identified in the product gas. High selectivity towards H_2 and CO were found for all catalysts and plasma-only, with a H_2/CO molar ratio of ~0.9. The lowest syngas selectivity was obtained with Cu/Al_2O_3 (~66%), which instead, had the highest alcohol selectivity (~3.6%).

1. Introduction

The emission of greenhouse gases, such as CO_2 and CH_4 related to the use of fossil fuels, is causing growing concern about global warming [1]. Reforming of CH_4 with CO_2 to syngas, known as dry reforming (Reaction (1)), is a possible way to remove the greenhouse gases and utilize CO_2 as a carbon resource [2]. The produced syngas consists of a mixture of H_2 and CO and is used as feedstock in a range of chemical processes, such as the Fischer-Tropsch synthesis [3] and methanol synthesis [4,5].

$$CH_4 + CO_2 \rightarrow 2CO + 2H_2,\ \Delta H_{R1} = 247\ \text{kJ/mol} \quad \text{(R1)}$$

To achieve substantial conversion and low carbon formation, a temperature of around 800 °C is usually applied, as carbon formation is thermodynamically favored in the temperature range of 560–700 °C [6–8]. Addition of a catalyst to the reforming reaction is required to facilitate the process, and focus has been on the use of supported noble metals (Rh, Ru, Pt, and Pd) as well as non-noble metals, mainly Ni, which is used industrially. The most common support materials are Al_2O_3, SiO_2, ZrO_2, and La_2O_3 [9].

A possible technology to remove the need for external heating, while simultaneously minimizing the carbon formation in dry reforming, is to use a non-thermal plasma (NTP). Combining catalysis with NTP, so-called plasma catalysis, is gaining increasing interest [10,11]. Several plasma types can be categorized as NTP, but the dielectric-barrier discharge (DBD) is the most widely applied for plasma catalysis [12]. A DBD reactor is typically arranged in a planar or cylindrical configuration with the discharge in the gap between the

* Corresponding author.
E-mail address: Aj@kt.dtu.dk (A.D. Jensen).

https://doi.org/10.1016/j.cej.2020.125519
Received 21 April 2020; Received in revised form 13 May 2020; Accepted 14 May 2020
Available online 17 May 2020
1385-8947/

electrodes [13]. In NTP, the freely moving electrons are characterized by a much higher temperature than the gas molecules, resulting in a mixture that is in non-thermodynamic equilibrium [12]. The high energy electrons collide with the gas molecules and form a range of species, including positive and negative ions, dissociated fragments such as free radicals, and electronically or vibrationally excited states of radicals and molecules [11]. This allows alternative reaction paths and formation of products that normally are unfavorable. The use of a NTP has been shown to convert the dry reforming mixture into syngas and valuable chemicals at atmospheric pressure and near room temperature [14–16].

NTP-based processes can be powered by renewable electricity from wind, hydro, or solar power and store this in a chemical form, as the flexibility of the plasma towards rapid start-up/shutdown allows operation that accommodates the fluctuations from such sources [12]. However, a trade-off between the conversion of reactants and the energy efficiency has been reported for many plasma systems [17,18]. Thus, the development of plasma chemical processes with high energy efficiency remains a challenge to be solved.

One strategy for optimizing the energy efficiency is to insert a solid packing in the discharge region to modify the plasma behavior and/or act as a catalyst in the plasma-mediated conversion. In recent years, the combined use of a DBD and catalysts has been subject of investigation for the conversion of CO_2 and CH_4, and various materials have been examined for plasma-catalytic dry reforming [19–24]. Na-ZSM-5 was demonstrated to effectively convert CH_4 and CO_2 in combination with plasma, but a large fraction of the product (i.e., 46%) was reported as unknown [19]. γ-Al_2O_3 impregnated with different catalytically active metals for DBD-based dry reforming was investigated by Zeng et al. [20]. They found that Ni, Co, and Cu catalysts showed slightly lower CO_2 conversion (8–9%) compared to plasma without catalytic packing (10%), while a Mn catalyst showed a similar level. All of the catalysts showed improved CH_4 conversion with Ni yielding the highest degree (19.5%) [20]. A different trend was reported by Tu et al. [21] when introducing Ni/Al_2O_3 into the plasma. Here the conversion of both CH_4 and CO_2 decreased compared to the situation without packaging. It was further reported that a transition occurred in the discharge behavior from a typical filamentary discharge when no packing was present to a combination of surface discharges and spatially limited microdischarges when the discharge region was fully packed. It was concluded that the size, shape, and volume fraction of the packed material influences the discharge type. Wang et al. [22] performed DBD-based dry reforming using γ-Al_2O_3 impregnated with Cu, Au, or Pt, and again, none of the tested plasma-catalyst combinations surpassed the conversion of CH_4 and CO_2 obtained without packing (~18% for CH_4 and ~15.5% for CO_2). However, high selectivities of liquid products were observed. This was attributed to the novel design of the DBD reactor, using a grounded water electrode [22]. A recent study on dry reforming in DBD plasma by Michielsen et al. [25] showed that packing the discharge region with oxides typically used as support material for catalysts (ZrO_2, SiO_2, α-Al_2O_3, γ-Al_2O_3, and $BaTiO_3$) significantly affected the conversion and product selectivity. It was reported that the use of α-Al_2O_3 resulted in the highest CO_2 (23%) and CH_4 (33%) conversion with a high CO selectivity, while SiO_2 improved the C_2 selectivity, and $BaTiO_3$ showed higher selectivity towards oxygenates [25]. Thus, it is clear that various contradictory observations have been reported in literature regarding both the product spectrum and the efficiency of the catalytic material. This shows that there is still much to learn on the influence of solid (catalytic) materials in plasma driven processes such as dry reforming.

In this work, a DBD reactor was used to convert CO_2 and CH_4 into syngas at conditions where the plasma itself causes a significant conversion. The influence of loading 10 wt% of Ag and Cu and 1 wt% Pt on γ-Al_2O_3 spheres was evaluated in terms of conversion, product selectivity, and energy efficiency. X-ray diffraction (XRD) and scanning electron microscopy (SEM) have been used to characterize the fresh and spent catalysts.

2. Experimental

2.1. DBD setup

The reaction between CH_4 and CO_2 was carried out in a coaxial packed-bed DBD reactor with alumina as the dielectric-barrier (reactor wall). The outside of the reactor was covered by a 10 cm long stainless steel mesh, working as the outer electrode. A stainless steel rod with an outer diameter of 8 mm was used as the inner electrode. The inner diameter of the reactor tube was 17 mm, resulting in a discharge gap of 4.5 mm and a discharge volume of 17.7 cm^3. The outer diameter of the reactor was 21.8 mm, corresponding to a barrier thickness of 2.4 mm.

The inner electrode was grounded, while a high voltage powered the outer electrode. The power was supplied by a high voltage amplifier (TREK, model 20/20C-HS), which was controlled by a function generator (Tektronix, AFG1022). A fixed frequency of 3 kHz and plasma power of 45 W were used for all experiments. The applied voltage was measured with a high voltage probe (Tektronix, P6015A) attached on the outer electrode, while the total current was measured with a Rogowski coil (Pearson, 4100) on the grounding line. Additionally, the voltage drop over an external capacitor (10 nF), connecting the inner electrode and ground, was measured by a low voltage probe (Picotech, TA150) to obtain the generated charges (Q) in the plasma. All signals were recorded by a digital oscilloscope (Picotech, Picoscope 3405B) for continuous measurement of plasma power.

A gas mixture consisting of 25 Nml/min CH_4 (99.995%) and 25 Nml/min CO_2 (99.996%) was fed to the reactor by Bronkhorst mass flow controllers and the reactor effluent was analyzed using an online gas chromatograph (Thermo Fisher Trace 1300 GC) equipped with a flame ionization detector (FID) and a thermal conductivity detector (TCD). Each experiment was repeated three times to account for uncertainties such as randomness in the reactor packing, with a minimum of three GC measurements of the gaseous product. For the plasma catalysis experiments, the reactor discharge volume (17.7 cm^3) was filled with catalytic material, corresponding to approximately 11 g of material. The packing was held in place by glass wool on each side of the bed, just outside of the discharge zone. Dense packing of the reactor was ensured by utilizing a vibrational step.

Blank measurements were conducted prior to ignition of the plasma, which were used to determine the feed concentrations of CH_4 and CO_2. Besides the CH_4 and CO_2, 10 Nml/min of N_2 was added to the effluent between the reactor exit and the GC. The N_2 was used as an internal standard. All experiments were conducted at atmospheric pressure and with no addition of thermal heat. After ignition of the plasma, a period of 1 h was used to stabilize the power input, after which sampling was conducted. The conditions used in this work are summarized in Table 1.

2.2. Catalyst material

For the experiments with a catalytic packing material, non-

Table 1
Utilized operating conditions.

Parameter	Specification
Gap size (mm)	4.5
Discharge length (cm)	10
Plasma power (W)	45
Frequency (kHz)	3.0
Gas flow rate (Nml/min)	50
CH_4:CO_2 (mol/mol)	1:1
Diameter of catalytic material (mm)	3.5 – 4.4
Temperature	Ambient (no external heating)
Pressure	Atmospheric (~ 1.16 atm)

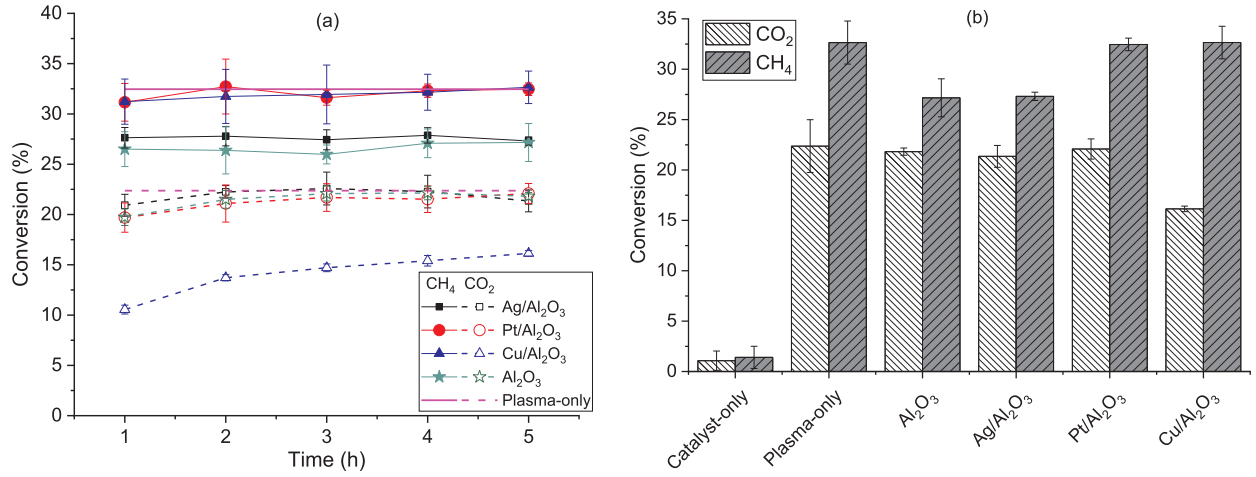

Fig. 1. Conversion of CH_4 and CO_2 as (a) function of time (repetitive use) for different catalyst packings and (b) effect of different operating modes (catalyst-only and plasma-only obtained after 1 h) and different catalyst packings after 5 h in plasma (CO_2/CH_4 = 1:1, total feed flow rate 50 Nml/min, plasma power 45 W at 3 kHz).

impregnated and impregnated γ-Al_2O_3 spheres were used. The diameter of the spheres was in the range of 3.5–4.4 mm. The coating of the spheres was performed by incipient wetness impregnation using nitrate salts as the metal precursors followed by calcination. The resulting materials used were 10 wt% Ag/Al_2O_3, 10 wt% Cu/Al_2O_3, and 1 wt% Pt/Al_2O_3.

Before using the catalytic material, it was treated in an argon–hydrogen plasma with 20 vol% of hydrogen and a total flow rate of 50 Nml/min for 30 min to pre-reduce the metals. The power used was 45 W at a frequency of 3 kHz, which is similar to the operating condition used during the dry reforming. Previous work has shown that supported metal oxide catalysts similar to these can be reduced in a low temperature argon–hydrogen plasma [26]. The effectiveness of the plasma pre-reduction is discussed in Section 3.2.

2.3. Measurement of conversion, product selectivity, energy cost, and energy efficiency

Each experiment was evaluated by analyzing the signals recorded by the oscilloscope and the GC. The conversion (X) of CH_4 and CO_2 are defined according to Eqs. (1) and (2). The selectivity (S) of a given product is calculated according to Eqs. (3) and (4) (i.e., H-based selectivity for H_2 and C-based selectivity for the other products).

$$X_{CH_4}(\%) = \frac{\text{Moles of } CH_{4in} - \text{Moles of } CH_{4out}}{\text{Moles of } CH_{4in}} = \frac{CH_{4converted}}{CH_{4in}} \quad (1)$$

$$X_{CO_2}(\%) = \frac{\text{Moles of } CO_{2in} - \text{Moles of } CO_{2out}}{\text{Moles of } CO_{2in}} = \frac{CO_{2converted}}{CO_{2in}} \quad (2)$$

$$S_{H_2}(\%) = \frac{H_{2produced}}{2 \cdot CH_{4converted}} \quad (3)$$

$$S_{C_xH_yO_z}(\%) = \frac{x \cdot C_xH_yO_z\ produced}{CH_{4converted} + CO_{2converted}} \quad (4)$$

The carbon balance (CB) is defined as the sum of carbon determined in each compound in the product gas divided by the sum of the moles of CH_4 and CO_2 in the inlet gas. The hydrogen balance (HB) and oxygen balance (OB) are determined in the same manner.

The energy efficiency of the reforming reaction (E) is defined as the moles of gas converted, divided by the plasma power, while the specific energy input (SEI) is the plasma power over the total flow rate [23]. A SEI of 54 J/ml was used throughout this work.

$$E(\text{mmol/kJ}) = \frac{CH_{4converted} + CO_{2converted}}{\text{Plasma power}} \quad (5)$$

$$SEI(\text{J/ml}) = \frac{\text{Plasma power}}{\text{Total flow rate}} \quad (6)$$

In addition, we defined an energy efficiency (η) based on the SEI and the reaction enthalpy (Δ_rH_i) of the two major reactions occurring in this study, i.e., dry reforming (Reaction (1)) and non-oxidative coupling of CH_4 into C_2H_6 (Reaction (2)). Note that this is only possible when the CO_2 conversion is the limiting conversion for the dry reforming reaction and when CO_2 and CH_4 is added in an equimolar ratio. The additional CH_4 conversion is then assumed to proceed in the formation of C_2H_6 (Reaction (2)). This other definition of energy efficiency, often used in plasma conversion experiments [12], is calculated by Eq. (7).

$$2CH_4 \rightarrow C_2H_6 + H_2,\ \Delta H_{R2} = 65.9\text{kJ/mol} \quad (R2)$$

$$\eta(\%) = \frac{X_{CO_2} \cdot \Delta H_{R1} + (X_{CH_4} - X_{CO_2}) \cdot \frac{\Delta H_{R2}}{2}}{SEI \cdot 24.46 \frac{1}{\text{mol}}} \cdot 100 \quad (7)$$

3. Results and discussion

3.1. Dry reforming at different operating modes

After the catalytic material was used in the plasma for one hour, the plasma and feed gas were turned off during analysis with the GC. After analysis, the gas flow was readmitted and the plasma reignited with the same packing in the discharge zone, which then was used for another hour. The same packing was used five times (5 h) before the reactor was emptied. This plasma on/off mode simulates the potential use of plasma catalysis with a fluctuating power source such as wind or solar energy.

Fig. 1(a) shows the conversion of CH_4 and CO_2 as a function of time for the four catalysts tested. No significant change in the CH_4 conversion is observed over the repeated use. However, for the CO_2 conversion, an initial increase in conversion is observed for all the catalysts, after which a stable conversion in the range of 20–22% is obtained, except for Cu/Al_2O_3. This catalyst showed an increase in CO_2 conversion over the 5 h period from 10.5% to 16.1%. The conversions obtained from plasma-only are included in Fig. 1(a) for comparison. The plasma-only experiments were only performed for one hour, as no changes in the system were expected.

Fig. 1(b) summarizes the conversion of the reactants in dry reforming when using catalyst-only (no electrical energy used), plasma-only, and plasma catalysis. The catalyst-only experiments were conducted as a blank run for an hour, and within the uncertainty no conversion is observed. This is as expected from the severe kinetic and thermodynamic limitations at this low temperature [17]. On the other

hand, when applying the 45 W plasma, a conversion of ~22% and ~33% for CO_2 and CH_4 is achieved.

The introduction of catalytic material is not found to increase the conversion of the two reactants. For the Al_2O_3, Ag/Al_2O_3, and Pt/Al_2O_3, the CO_2 conversion is similar to the plasma-only, while a decrease to 16% conversion is seen for the Cu catalyst. Similar results were reported by Wang et al. [22], where a 15 wt% Cu/Al_2O_3 catalyst showed low (7.5%) CO_2 conversion and a CH_4 conversion matching that of the plasma-only. Similarly to Wang et al., both the Cu and Pt catalysts are here observed to yield a CH_4 conversion close to the plasma-only mode, whereas the Al_2O_3 and Ag/Al_2O_3 show lower CH_4 conversion (Fig. 1). The lower conversion can be explained by the shorter residence time of the gas when introducing the packing. On the other hand, the packing increases the electrical field at the contact points, and thus also the electron temperature, which may result in enhanced dissociation by electron impact reactions, for the same plasma power [27]. Both effects compete with each other, but under the tested conditions, apparently the electric field enhancement is insufficient to compensate for the decrease in residence time.

Reaction (1) requires a stoichiometric conversion of CO_2 and CH_4. However, a higher CH_4 conversion is observed for both the plasma-only mode and the plasma-catalyst mode (Fig. 1), indicating that other reactions also occur. Previous publications testing different packing materials have reported the same [19,28]. These findings correlate with the threshold energies of direct electron-impact dissociation of CO_2 and CH_4 as presented in Reaction (3) and (4), which are 11 and 9 eV, respectively [29].

$$CO_2 + e \rightarrow CO + O + e \quad \text{(R3)}$$

$$CH_4 + e \rightarrow CH_3 + H + e \quad \text{(R4)}$$

3.2. Catalyst characterization by XRD

Fig. 2 shows the XRD patterns of the fresh and spent samples measured ex situ. The pattern of the γ-Al_2O_3 support shows three peaks located at 2θ = 37.8°, 43°, and 68.2°. These peaks also appear in the XRD patterns of the fresh and spent M/Al_2O_3 (M = Ag, Cu, and Pt) catalysts. The XRD pattern of both the fresh and spent Pt/Al_2O_3 shows one weak reflection peak (39.8°). The Pt is almost certainly amorphous and the peaks therefore most likely correspond to PtO_2 in the fresh catalyst and to Pt in the spent sample. For the Cu/Al_2O_3 fresh catalyst, peaks are observed at 35.5°, 38.7°, 48.9°, and 61.6°, consistent with CuO, while the spent Cu/Al_2O_3 catalyst has metallic Cu peaks at 43.4° and 50.5° and a weak CuO peak at 35.5°. Lastly, the fresh Ag/Al_2O_3 catalyst shows peaks corresponding to Ag_2CO_3 (19.4°, 33.7°, 48.5° and 60.5°) and Ag_2O (32.9° and 38.1°), while peaks consistent with metallic Ag (38.2°, 44.3°, and 64.5°) are observed for the spent Ag/Al_2O_3 catalyst. A general transition from oxides to metals is therefore observed for the spent catalysts. Although the ex situ nature of the XRD analyses should be acknowledged, the existence of remaining CuO in the spent catalyst sample suggests that complete reduction was not achieved during the pre-reduction and reforming. This can explain why the Cu-based sample exhibits a lower and gradually increasing apparent CO_2 conversion in Fig. 1. The CO_2 conversion will appear lower as the formed CO reacts with the remaining CuO and regenerates the CO_2 as shown in R5. As time progresses the CuO is gradually removed and more CO will pass through unreacted, resulting in a steadily increasing apparent CO_2 conversion.

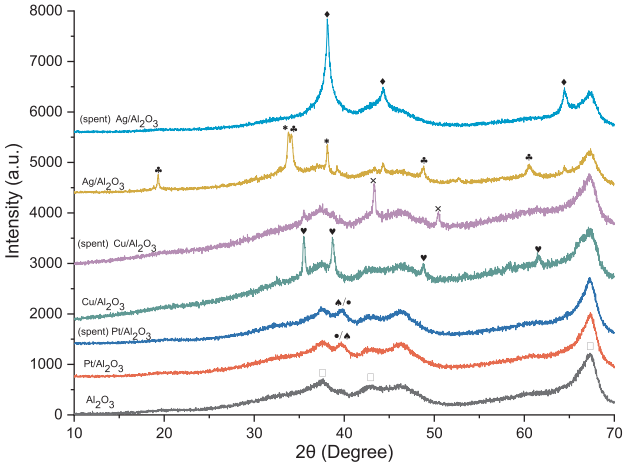

Fig. 2. XRD patterns of fresh and spent catalytic material (♦Ag, ♣Ag_2CO_3, *Ag_2O, × Cu, ♥CuO, ♠ Pt, •PtO_2, □Al_2O_3).

$$CO + CuO \rightarrow Cu + CO_2 \quad \text{(R5)}$$

3.3. Product distribution

The primary identified products from the dry reforming are CO and H_2 as shown in Fig. 3(a). The catalytic materials only have a modest impact on the CO and H_2 selectivities with Al_2O_3 and Ag/Al_2O_3 giving slightly higher selectivities and Pt/Al_2O_3 and Cu/Al_2O_3 giving slightly lower selectivities than the plasma-only. Interestingly, Al_2O_3 shows the highest H_2 selectivity, which is in agreement with observations in the literature for similar catalytic materials [22].

A H_2/CO molar ratio of 1 is dictated for pure dry reforming (Reaction (1)), which is in reasonable agreement with the observed ratios (see Fig. 3(b)). However, the higher conversion of CH_4 compared to CO_2 indicates that more H_2 could have been formed compared to CO, while the H_2/CO ratio is slightly below 1. This suggests that CH_4 is also partially converted into larger hydrocarbons, as indicated by Fig. 3(c). In addition, as discussed above, our results indicate that if the metal oxides have not been completely reduced before the reforming reaction, the formed CO may react with the oxide. This removes the produced CO, which results in a higher H_2/CO molar ratio. The XRD results in Fig. 2 indicate that this is most important for the Cu/Al_2O_3 sample and this is most likely the reason why the H_2/CO ratio for this sample is considerably higher than for plasma-only and for the other catalysts (see Fig. 3(b)). It is therefore of great importance to fully reduce the metal oxides before the reforming takes place.

It is worth mentioning that H_2/CO ratios in the range of 0.1–0.2 have been reported by Michielsen et al. [25], when using a comparable setup to this study (major differences were a plasma power of 62 W at a frequency of 23.5 kHz, and sphere size of 1.25–2.24 mm). Tuning of the plasma parameters, such as power and frequency, along with the physical parameters of the setup (gap size, discharge length, dielectric-barrier material, packing degree, etc.) might thus have a significant influence on the selectivity, indicating that not only the packing material can modify the product distribution.

Besides CO and H_2, a variety of saturated and unsaturated hydrocarbons were detected from the dry reforming, along with oxygenated compounds, as presented in Fig. 3(c). The selectivity towards ethane and propane was by far the highest among the detected by-products, with C-based selectivities above 10% for ethane and above 3% for propane. Packing the discharge zone with Al_2O_3 or Ag/Al_2O_3 resulted in the highest selectivity for ethane (11.8%), while the plasma only gave the highest selectivity to propane (3.9%). The relatively high selectivity towards ethane supports the above suggestion of CH_4 dissociation to methyl radicals, that recombine to form ethane [30,31]. It is interesting to note that methanol is the fifth most selective compound, and for the Cu/Al_2O_3 catalyst, the selectivity reached a value of ~3.2%. The formation of methanol most likely occurs through reaction between a methyl radical and a hydroxyl radical, formed from a free hydrogen and oxygen radical [32].

The selectivity of C_2 hydrocarbons, C_{3+} hydrocarbons, and alcohols

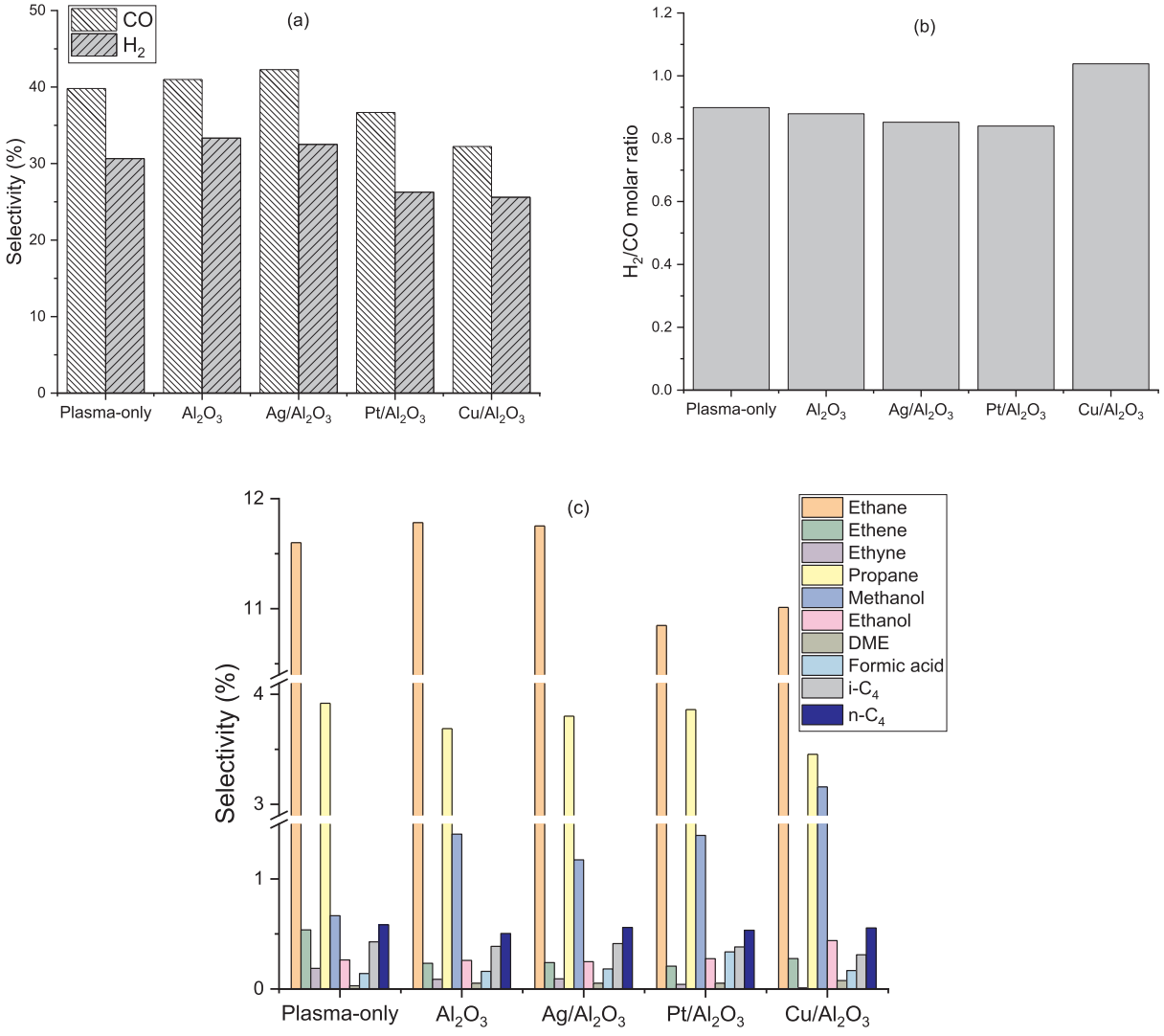

Fig. 3. Effect of different catalysts on (a) selectivity to H_2 and CO; (b) H_2/CO molar ratio; (c) selectivity to different hydrocarbons and oxygenates. The measurements with catalysts are obtained after 5 h in plasma, while the plasma-only results were recorded after 1 h (CO_2/CH_4 = 1:1, total feed flow rate 50 Nml/min, plasma power 45 W at 3 kHz).

was also measured as a function of time. Only small changes were observed, as indicated in the supplementary material (Fig. S1). However, one remarkable change was observed for the alcohol selectivity with the Cu catalyst. Indeed, an increase from 1.1% to 3.6% over the five-hour period was seen, which is likely a consequence of the emerging metallic Cu sites as the CuO is gradually reduced. It is well known that a Cu/Al_2O_3 catalyst can be used for thermal-catalytic formation of methanol in a $CO_2/CO/H_2$ mixture [5].

The remaining detected compounds are formed with a selectivity lower than 1%. The selectivity to the two C_4 compounds are determined based on the effective carbon method proposed by Schofield [33], using propane as the reference compound. Many small undetermined peaks were observed on the FID signal from the GC, meaning that even more species are being formed in the DRM, giving a very complex product mixture. This is also reflected in the elemental balances (Fig. S2), as a considerable deviation in the closure of the balances is found. The poor closure of the mass balances suggests a selectivity of 39–48% towards unidentified carbon-containing species (Table S1). This conclusion is supported by the GC measurements on the internal N_2 standard, which show that no volume expansion occurs, despite this being expected from Reaction (1). This shows that unidentified higher molecular weight products are formed that compensates for the volume expansion expected from Reaction (1). Concerning the nature of these unidentified products, the mass balances indicate a product with an equal atom number of carbon and oxygen and slightly higher number of hydrogen atoms. This could be products such as formaldehyde (CH_2O) or acetic acid (CH_3COOH), which were observed by Wang et al. [22] during investigations of plasma dry reforming at a lower power input, but were not identified in this study. Another possibility is the formation of solid carbon and H_2O.

Based on the observed selectivities (Fig. 3(c)), possible reaction pathways for the formation of alcohols and higher hydrocarbons under the utilized conditions are proposed in Scheme 1. O, H, CO, CH_3, and CH_2 are suggested to be key species in the plasma dry reforming reactions [22,30–32]. It is further proposed that ethane is an intermediate in the formation of propane and CH_2OH and formate are intermediates for the formation of methanol. For ethane to proceed to propane a hydrogen atom must be abstracted by an electron impact, while CH_2OH and formate must react with a hydrogen radical to form methanol. The ethane and propane selectivities are relatively unaffected by the implementation of a solid packing material, indicating that these reactions occur in the gas phase and are determined by electron impact frequencies. On the other hand, the methanol selectivity is highly dependent on the solid packing, suggesting that parts of the pathway must

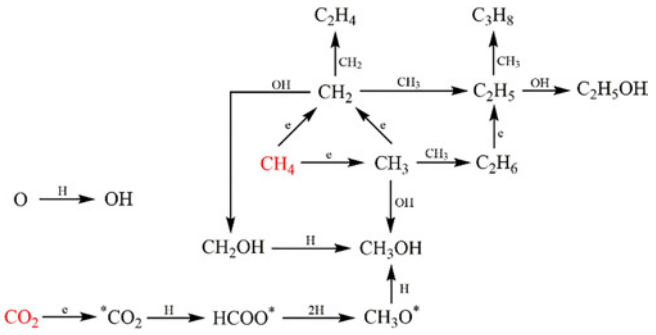

Scheme 1. Overview of possible reaction pathways for the conversion of CH_4 and CO_2 into alcohols and higher hydrocarbons in plasma dry reforming of methane with a DBD reactor. * indicates an energized molecule.

Fig. 4. Image of fresh (left) and spent (right) Al_2O_3.

take place on the surface of the catalysts. The CO_2 conversion to methanol could be catalyzed by the Cu/Al_2O_3 through formate, similarly to thermo-catalysis [4,34,35], contributing to the 475% increase in methanol selectivity for this catalyst compared to plasma-only.

Apart from the solid packing materials raising the methanol selectivity and the higher H_2/CO ratio for Cu/Al_2O_3, which was attributed to produced CO reacting with residual CuO in the sample, the solid materials have very little impact on the conversion and product distribution. Similar observations were made by Song et al. [24]. Their study concluded the loading weight of Ni on γ-Al_2O_3 had no effect on the conversion and product distribution at a power input of 130 W. This indicates that the plasma is dominating the events at elevated power inputs. Studying the effect of particle size, plasma power, frequency, and loading of active material at lower plasma power will therefore be important to optimize the plasma-catalytic dry reforming.

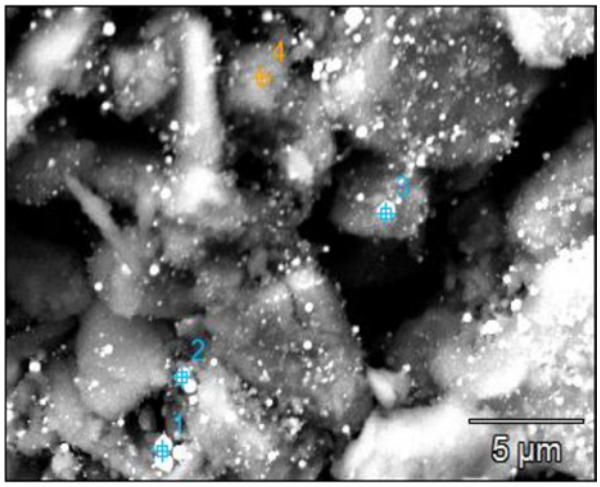

Fig. 6. SEM image of spent Al_2O_3 with analysis points.

Table 2
Measured composition at analysis locations shown on Fig. 6.

Weight %	O	Al	Cr	Fe	Ni
Location 1	5.1	25.2	11.6	50.6	6.1
Location 2	10.6	67.7	4.6	17.1	
Location 3	2.4	77.3	4.3	14.6	
Location 4	38.5	56.5	0.9	3.5	

Table 3
Summary of results.

Catalyst	Conversion (%)		H_2/CO	E (mmol/kJ)	η (%)
	CH_4	CO_2			
None (plasma-only)	32.6	22.4	0.899	0.206	4.44
Al_2O_3	27.2	21.8	0.879	0.185	4.16
Ag/Al_2O_3	27.3	21.4	0.852	0.183	4.14
Pt/Al_2O_3	32.5	22.1	0.840	0.205	4.39
Cu/Al_2O_3	32.6	16.1	1.04	0.185	3.43

3.4. Analysis of spent catalyst

All the spent solids containing metals (Ag, Pt, and Cu) were blackened after the reforming tests, indicating the formation of carbon deposits. Interestingly, the spent Al_2O_3 samples only showed intense

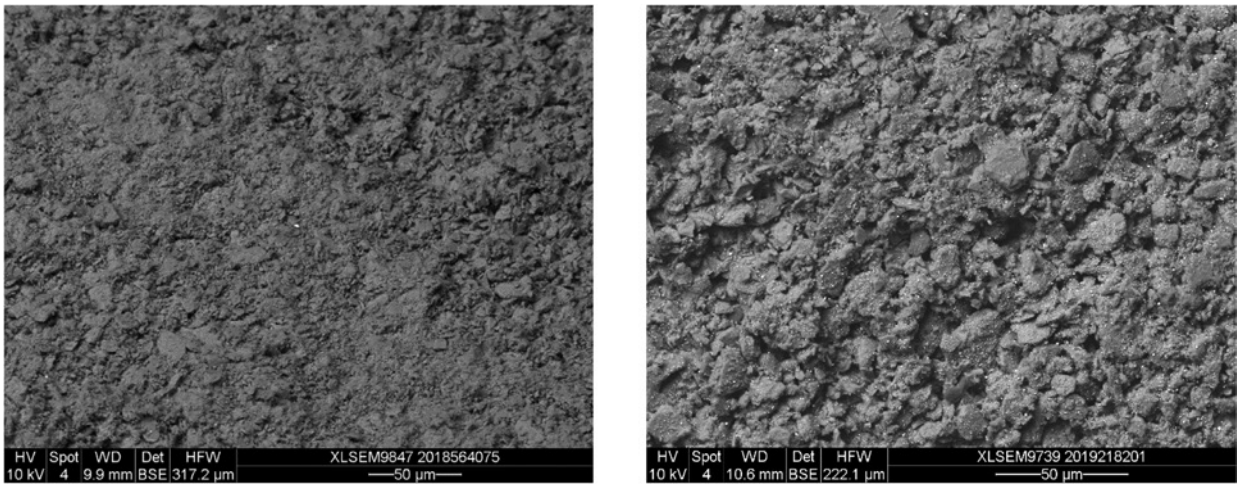

Fig. 5. SEM image of fresh (left) and spent (right) Al_2O_3.

Table 4
Energy efficiency of DBD dry reforming.

Packing	CH_4:CO_2	Total gas flow rate (ml/min)	Power (W)	Conversion (%)		E (mmol/kJ)	Ref
				CH_4	CO_2		
$LaNiO_3$	1:1	50	160	64	55	0.14	[36]
$LaNiO_3$@SiO_2	1:1	40	150	88	78	0.17	[37]
None	1:1	50	45	33	22	0.21	This work
Ni-K/Al_2O_3*	3:2	50	16	32	23	0.67	[38]
Ni/Al_2O_3	1:1	50	7.5	20	9.3	0.72	[20]
Ni-Mn/Al_2O_3	1:1	30	2.1	28	12	2.2	[23]

*External heating to 160 °C used.

discoloring around what is expected to be the contact point with the electrode (see Fig. 4). The dark color could be removed by heating in the presence of oxygen, suggesting that the dark color is due to carbonaceous deposits.

SEM images of the fresh and spent Al_2O_3 showed no remarkable change, indicating that the plasma does not inflict modifications to the alumina morphology (see Fig. 5). SEM images of the remaining catalytic materials tested are shown in the supplementary material and show no morphological differences between fresh and spent samples either. However, energy-dispersive X-ray spectroscopy (EDS) analysis of the discolored surface region in the spent Al_2O_3 revealed traces of Fe, Cr, and Ni, indicating that the material from the inner electrode had migrated to the sample surface (see Fig. 6 and Table 2).

For all the catalysts, the darkening attributed to carbon deposition is correlated to metal content - either metals pre-deposited on the Al_2O_3 or metal particles migrating to the alumina from the electrode during the discharge. These observations suggest that at the present conditions, where the energy input is so high that the plasma itself mainly facilitates the reforming, the metallic surfaces interact so strongly with the adsorbates that for the most part decomposition and carbon deposition occurs. The carbon formation therefore most likely blocks the sites and prevents further reaction, which could be part of the explanation for the similar selectivities seen in Fig. 3.

3.5. Energy efficiency

The effect of performing the plasma dry reforming with different catalytic materials on the energy efficiency (both E and η) is shown in Table 3. The plasma-only and the Pt/Al_2O_3 packing yield similar efficiencies, i.e., 0.206 and 0.205 mmol/kJ, or 4.44 and 4.39%, respectively, which is a result of the comparable conversions, while the other catalysts yield a slightly lower conversion, and thus a somewhat lower energy efficiency. Table 4 compares the energy efficiency of DBD-based dry reforming reported in literature. The energy efficiency achieved in this work is relatively low compared to other studies, as no synergy between the tested materials and the plasma was observed at these conditions. As shown in Table 4, a higher energy efficiency is generally observed at lower plasma power. More research at lower power values could therefore be important to find a more efficient plasma-catalytic combination.

The calculated energy efficiency from Eq. (7) (η) is a measure for how much energy is used in the conversion of CH_4 and CO_2 based on the resulting products. However, the product mixture is complex as shown in Fig. 3, which means that a wide range of reactions occur in the plasma. This means that this energy efficiency can only give an estimate. Nevertheless, calculating the energy efficiency in this manner provides an easy comparison with other technologies and their efficiency in storing electrical energy. From Table 3, it is seen that only ~4% of the energy input is utilized in the conversion of the reactants. This low utilization is a major drawback for the DBD technology and must be improved through further investigation of plasma/catalyst/setup combinations.

4. Conclusion

Plasma-based dry reforming has been carried out in a coaxial DBD reactor at ambient pressure and temperature with and without catalytic packing material. It was shown that the plasma is able to activate the dry reforming feed mixture at ambient conditions and alone achieved a conversion of ~33% for CH_4 and ~22% for CO_2. Presence of a catalyst in the discharge zone led to a somewhat lower conversion of the two reactants for most catalysts, except for Pt/Al_2O_3, for which the conversion was similar to the plasma-only. This means that the electric field enhancement near the contact points of the packing beads, which may give rise to enhanced dissociation, cannot compensate for the shorter gas residence in the plasma due to the packing, at the conditions of this study. The use of Al_2O_3 and Ag/Al_2O_3 packing showed similar CO_2 conversion as Pt/Al_2O_3, but lower CH_4 conversion, while Cu/Al_2O_3 showed the opposite trend. From XRD of the spend sample, insufficient reduction of CuO was detected, which could explain the low CO_2 conversion.

H_2 and CO were found to make up 66–77% of the formed products on a mole basis. However, a large variety of saturated and unsaturated hydrocarbons as well as oxygenated compounds were detected in the dry reforming products. Among these, ethane, propane, and methanol were formed with the highest selectivity. Similar selectivities were observed for the different catalytic materials indicating that the catalytic activity was not significant compared to the plasma effect.

Signs of electrode decomposition was observed from SEM-EDS analysis, as traces of Fe, Ni, and Cr were seen on the spent Al_2O_3 sample surface. Increased black discoloring was observed in the areas of migration, indicating that the addition of metal sites on the Al_2O_3 surface increases the formation of solid carbon.

A relatively low energy efficiency was observed in this study with no apparent synergy between the tested catalytic materials and the plasma. Indeed, only 4% of the plasma power was used for the conversion of the reactants. We expect that a lower plasma power will result in better energy efficiency.

Declaration of Competing Interest

The authors declare that they have no known competing financial interests or personal relationships that could have appeared to influence the work reported in this paper.

Acknowledgments

We thank Haldor Topsoe A/S for providing all the catalytic materials used and the Department of Chemical and Biochemical Engineering, Technical University of Denmark, for funding this project.

Appendix A. Supplementary data

Supplementary data to this article can be found online at https://doi.org/10.1016/j.cej.2020.125519.

References

[1] E.A. Rosa, T. Dietz, Human drivers of national greenhouse-gas emissions, Nat. Clim. Chang. 2 (2012) 581–586, https://doi.org/10.1038/nclimate1506.

[2] A.T. Ashcroft, A.K. Cheetham, M.L.H. Greent, P.D.F. Vernont, Partial oxidation of methane to synthesis gas using carbon dioxide, Nature. 350 (1991) 225–226.

[3] A. Demirbas, Methane Gas Hydrate – Green Energy and Technology, Springer London, 2010 doi:10.1007/978-1-84882-872-8.

[4] N.D. Nielsen, J. Thrane, A.D. Jensen, J.M. Christensen, Bifunctional synergy in CO hydrogenation to methanol with supported Cu, Catal. Lett. 1 (2019) 1–7, https://doi.org/10.1007/s10562-019-03036-7.

[5] K.C. Waugh, Methanol synthesis, Catal. Lett. 142 (2012) 1153–1166, https://doi.org/10.1007/s10562-012-0905-2.

[6] P.M. Mortensen, I. Dybkjær, Industrial scale experience on steam reforming of CO_2-rich gas, Appl. Catal. A Gen. 495 (2015) 141–151, https://doi.org/10.1016/j.apcata.2015.02.022.

[7] M.-S. Fan, A.Z. Abdullah, S. Bhatia, Catalytic technology for carbon dioxide reforming of methane to synthesis gas, ChemCatChem. 1 (2009) 192–208, https://doi.org/10.1002/cctc.200900025.

[8] Y. Wang, L. Yao, S. Wang, D. Mao, C. Hu, Low-temperature catalytic CO_2 dry reforming of methane on Ni-based catalysts: a review, Fuel Process. Technol. 169 (2018) 199–206, https://doi.org/10.1016/j.fuproc.2017.10.007.

[9] Y.H. Hu, E. Ruckenstein, Catalytic conversion of methane to synthesis gas by partial oxidation and CO_2 reforming, Adv. Catal. 48 (2004) 297–345, https://doi.org/10.1016/S0360-0564(04)48004-3.

[10] E.C. Neyts, K. Ostrikov, M.K. Sunkara, A. Bogaerts, Plasma catalysis: synergistic effects at the nanoscale, Chem. Rev. 115 (2015) 13408–13446, https://doi.org/10.1021/acs.chemrev.5b00362.

[11] J.C. Whitehead, Plasma–catalysis: the known knowns, the known unknowns and the unknown unknowns, J. Phys. D. Appl. Phys. 49 (2016) 243001, , https://doi.org/10.1088/0022-3727/49/24/243001.

[12] R. Snoeckx, A. Bogaerts, Plasma technology - a novel solution for CO_2 conversion? Chem. Soc. Rev. 46 (2017) 5805–5863, https://doi.org/10.1039/c6cs00066e.

[13] U. Kogelschatz, B. Eliasson, W. Egli, From ozone generators to Flat television screens: history and future potential of dielectric-barrier discharges, Pure Appl. Chem. 71 (1999) 1819–1828.

[14] H.D. Gesser, N.R. Hunter, D. Probawono, The CO_2 reforming of natural gas in a silent discharge reactor, Plasma Chem. Plasma Process. 18 (1998) 241–245, https://doi.org/10.1023/A:1021602600113.

[15] L.M. Zhou, B. Xue, U. Kogelschatz, B. Eliasson, Nonequilibrium plasma reforming of greenhouse gases to synthesis gas, Energy Fuels. 12 (1998) 1191–1199, https://doi.org/10.1021/ef980044h.

[16] N. Seyed-Matin, A. Hossein Jalili, M. Hosseini Jenab, S. Majid Zekordi, A. Afzali, C. Rasouli, A. Zamaniyan, DC-pulsed plasma for dry reforming of methane to synthesis gas, Plasma Chem Plasma Process. 30 (2010) 333–347, https://doi.org/10.1007/s11090-010-9225-8.

[17] X. Tu, J.C. Whitehead, Plasma-catalytic dry reforming of methane in an atmospheric dielectric barrier discharge: understanding the synergistic effect at low temperature, Appl. Catal. B Environ. 125 (2012) 439–448, https://doi.org/10.1016/j.apcatb.2012.06.006.

[18] X. Zheng, S. Tan, L. Dong, S. Li, H. Chen, Plasma-assisted catalytic dry reforming of methane: Highly catalytic performance of nickel ferrite nanoparticles embedded in silica, J. Power Sources. 274 (2015) 286–294, https://doi.org/10.1016/j.jpowsour.2014.10.065.

[19] K. Krawczyk, M. Młotek, B. Ulejczyk, K. Schmidt-Szałowski, Methane conversion with carbon dioxide in plasma-catalytic system, Fuel. 117 (2014) 608–617, https://doi.org/10.1016/j.fuel.2013.08.068.

[20] Y. Zeng, X. Zhu, D. Mei, B. Ashford, X. Tu, Plasma-catalytic dry reforming of methane over γ-Al_2O_3 supported metal catalysts, Catal. Today. 256 (2015) 80–87, https://doi.org/10.1016/j.cattod.2015.02.007.

[21] X. Tu, H.J. Gallon, M.V. Twigg, P.A. Gorry, J.C. Whitehead, Dry reforming of methane over a Ni/Al_2O_3 catalyst in a coaxial dielectric barrier discharge reactor, J. Phys. D Appl. Phys. 44 (2011), https://doi.org/10.1088/0022-3727/44/27/274007.

[22] L. Wang, Y. Yi, C. Wu, H. Guo, X. Tu, One-step reforming of CO_2 and CH_4 into high-value liquid chemicals and fuels at room temperature by plasma-driven catalysis, Angew. Chemie. 56 (2017) 13679–13683, https://doi.org/10.1002/anie.201707131.

[23] D. Ray, P.M.K. Reddy, C. Subrahmanyam, Ni-Mn/γ-Al_2O_3 assisted plasma dry reforming of methane, Catal. Today. 309 (2018) 212–218, https://doi.org/10.1016/j.cattod.2017.07.003.

[24] H.K. Song, J.-W. Choi, S.H. Yue, H. Lee, B.-K. Na, Synthesis gas production via dielectric barrier discharge over Ni/γ-Al_2O_3 catalyst, Catal. Today. 89 (2004) 27–33, https://doi.org/10.1016/j.cattod.2003.11.009.

[25] I. Michielsen, Y. Uytdenhouwen, A. Bogaerts, V. Meynen, Altering conversion and product selectivity of dry reforming of methane in a dielectric barrier discharge by changing the dielectric packing material, Catalysts. 9 (2019) 51, https://doi.org/10.3390/catal9010051.

[26] X. Tu, H.J. Gallon, J.C. Whitehead, Plasma-assisted reduction of a NiO/Al_2O_3 catalyst in atmospheric pressure H_2/Ar dielectric barrier discharge, Catal. Today. 211 (2013) 120–125.

[27] K. Van Laer, A. Bogaerts, How bead size and dielectric constant affect the plasma behaviour in a packed bed plasma reactor: a modelling study, Plasma Sources Sci. Technol. 26 (2017), https://doi.org/10.1088/1361-6595/aa7c59.

[28] H.J. Gallon, X. Tu, J.C. Whitehead, Effects of reactor packing materials on H_2 production by CO_2 reforming of CH_4 in a dielectric barrier discharge, Plasma Process. Polym. 9 (2012) 90–97, https://doi.org/10.1002/ppap.201100130.

[29] W.-C. Chung, M.-B. Chang, Review of catalysis and plasma performance on dry reforming of CH_4 and possible synergistic effects, Renew. Sustain. Energy Rev. 62 (2016) 13–31, https://doi.org/10.1016/j.rser.2016.04.007.

[30] A.H. Khoja, M. Tahir, N.A.S. Amin, Recent developments in non-thermal catalytic DBD plasma reactor for dry reforming of methane, Energy Convers. Manag. 183 (2019) 529–560, https://doi.org/10.1016/j.enconman.2018.12.112.

[31] G. Scarduelli, G. Guella, D. Ascenzi, P. Tosi, Synthesis of liquid organic compounds from CH_4 and CO_2 in a dielectric barrier discharge operating at atmospheric pressure, Plasma Process. Polym. 8 (2011) 25–31, https://doi.org/10.1002/ppap.201000044.

[32] C. De Bie, J. Van Dijk, A. Bogaerts, The dominant pathways for the conversion of methane into oxygenates and syngas in an atmospheric pressure dielectric barrier discharge, J. Phys. Chem. C. 119 (2015) 22331–22350, https://doi.org/10.1021/acs.jpcc.5b06515.

[33] K. Schofield, The enigmatic mechanism of the flame ionization detector: Its overlooked implications for fossil fuel combustion modeling, Prog. Energy Combust. Sci. 34 (2008) 330–350, https://doi.org/10.1016/j.pecs.2007.08.001.

[34] M. Bowker, R.A. Hadden, H. Houghton, K. Waugh, The mechanism of methanol synthesis on copper/zinc oxide/alumina catalysts, J. Catal. 109 (1988) 263–273.

[35] Y. Amenomiya, T. Tagawa, Infrared study of methanol synthesis from CO_2 + H_2 on supported copper-zinc oxide catalysts, in, Proc. 8th Int. Cogr. Catal., Berlin (1984) 557–567.

[36] X.-G. Zheng, S.-Y. Tan, L.-C. Dong, S.-B. Li, H.-M. Chen, S.-A. Wei, Experimental and kinetic investigation of the plasma catalytic dry reforming of methane over perovskite $LaNiO_3$ nanoparticles, Fuel Process. Technol. 137 (2015) 250–258, https://doi.org/10.1016/j.fuproc.2015.02.003.

[37] X. Zheng, S. Tan, L. Dong, S. Li, H. Chen, $LaNiO_3$@SiO_2 coreeshell nano-particles for the dry reforming of CH_4 in the dielectric barrier discharge plasma, Int. J. Hydrogen Energy. 39 (2014) 11360–11367, https://doi.org/10.1016/j.ijhydene.2014.05.083.

[38] Y.X. Zeng, L. Wang, C.F. Wu, J.Q. Wang, B.X. Shen, X. Tu, Low temperature reforming of biogas over K-, Mg- and Ce-promoted Ni/Al_2O_3 catalysts for the production of hydrogen rich syngas: understanding the plasma-catalytic synergy, Appl. Catal. B Environ. 224 (2018) 469–478, https://doi.org/10.1016/j.apcatb.2017.10.017.